

Evidence for an iron-hydrogen complex in p-type silicon

S. Leonard,^{1,a)} V. P. Markevich,¹ A. R. Peaker,¹ B. Hamilton,¹ and J. D. Murphy²

¹Photon Science Institute, University of Manchester, Manchester M13 9PL, United Kingdom

²School of Engineering, University of Warwick, Coventry CV4 7AL, United Kingdom

(Received 9 April 2015; accepted 13 July 2015; published online 22 July 2015)

Interactions of hydrogen with iron have been studied in Fe contaminated p-type Czochralski silicon using capacitance-voltage profiling and deep level transient spectroscopy (DLTS). Hydrogen has been introduced into the samples from a silicon nitride layer grown by plasma enhanced chemical vapor deposition. After annealing of the Schottky diodes on Si:Fe + H samples under reverse bias in the temperature range of 90–120 °C, a trap has been observed in the DLTS spectra which we have assigned to a Fe-H complex. The trap is only observed when a high concentration of hydrogen is present in the near surface region. The trap concentration is higher in samples with a higher concentration of single interstitial Fe atoms. The defect has a deep donor level at $E_v + 0.31$ eV. Direct measurements of capture cross section of holes have shown that the capture cross section is not temperature dependent and its value is 5.2×10^{-17} cm². It is found from an isochronal annealing study that the Fe-H complex is not very stable and can be eliminated completely by annealing for 30 min at 125 °C. © 2015 AIP Publishing LLC. [<http://dx.doi.org/10.1063/1.4927323>]

Iron is a common impurity in silicon for photovoltaic applications.¹ It is one of the most harmful contaminants and has a strong detrimental effect on solar cell performance.^{1–3} The most energetically favorable location for a single Fe atom in the Si lattice is a tetrahedral interstitial site.⁴ Interstitial iron (Fe_i) in Si has a donor level at about $E_v + 0.38$ eV and large capture cross section for electrons that makes it a strong recombination center in p-type Si.^{1,5} Fe_i can diffuse in Si at room temperature and in p-type Si it forms complexes with shallow acceptor dopants.^{6,7} The iron-acceptor complexes can be dissociated upon annealing at temperatures higher than 100 °C or at room temperature under above band gap illumination.¹ Some cheaper “solar grade” silicon which is widely used for production of solar cells contains higher concentrations of Fe and other metallic impurities compared to “electronic grade” material. Due to the desire to be able to use cheaper silicon feedstock with a higher metallic content, the understanding of iron-related defects in the “solar grade” silicon and finding ways of their elimination or passivation are a hot topic of research.⁸

For crystalline silicon, there are very effective ways to getter Fe,⁹ but in multi-crystalline silicon the gettering techniques are less effective due to Fe decoration of grain boundaries and extended defects.¹⁰ For this reason, there has been a lot of interest in electrical passivation of Fe. Hydrogen is commonly used to passivate lifetime-limiting defects in silicon and is normally introduced into Si-based photovoltaic devices from the silicon nitride anti-reflection coating.¹¹ Several groups have used deep level transient spectroscopy (DLTS) to examine the effects of hydrogen on Fe in p-type silicon, but with no strong evidence of passivation or formation of Fe-H complexes with deep levels in the gap.^{12–15} This can be expected taking into account a well-known fact that both interstitial hydrogen and iron atoms are generally positively charged in p-type Si and so the Coulomb repulsion

of Fe_i and H prevents the formation of Fe-H complexes. In n-type silicon contaminated with iron, a hole trap with an energy level at about $E_v + 0.31$ eV was detected and assigned to a Fe-H defect.¹⁶ *Ab initio* calculations predicted that a Fe-H complex should be stable at room temperature and have a deep donor level at about $E_v + 0.40$ eV and a deep acceptor level at about $E_c - 0.3$ eV.¹⁷ Recently, there have been reports of the passivating effect of hydrogen on Fe in multi-crystalline silicon, with some publications showing that H does appear to have a strong and thermally stable passivating effect of iron in multi-crystalline silicon.^{18,19} However, this contradicts the conclusions of other studies which show the absence of H-induced Fe passivation.²⁰

Electronic grade boron doped Cz-Si wafers ($\sim 12 \Omega$ cm) were cleaved into ~ 5 cm \times 5 cm squares. The samples were rubbed with iron (99.95% purity from Testbourne Limited, UK) on the back side and then annealed in air in the temperature range of 790–875 °C in a pre-heated furnace for 24 h. The heat treatments were followed by rapid cooling (below 200 °C in <10 s) to room temperature.²¹ A surface iron silicide is formed as a result of this process²² and is removed with a planar etch comprising HF (40%), HNO₃ (69%), and CH₃COOH (glacial) in the ratio of 8:75:17. Samples were subjected to an HF dip, followed by an RCA clean and hydrogen was then introduced into the wafer from a silicon nitride layer grown by direct plasma enhanced chemical vapour deposition at 350 °C. The samples were left at room temperature for over a week, cut into smaller pieces, and then the silicon nitride layer was removed with diluted HF (10%). Schottky diodes were formed on the samples by sputtering Ti and Al through a shadow mask, and a layer of Au was thermally evaporated onto the back side to form an Ohmic contact. The samples with the Schottky diodes were annealed under vacuum in the temperature range of 50–175 °C with and without reverse bias. After reverse bias annealing (RBA), the samples were cooled down to lower temperatures for electrical measurements with the bias

^{a)}Email: simon.leonard@manchester.ac.uk

applied. Current-voltage and capacitance-voltage (C-V) measurements were undertaken at different temperatures to check the quality of the diodes, to determine the concentration of shallow uncompensated acceptors, and to determine the probing depths for capacitance transient measurements. DLTS and Laplace DLTS (LDLTS)²³ were used to characterize defects with deep electronic levels and determine the concentration of Fe_i related centers.

Fig. 1 shows the conventional DLTS spectra of two different Fe contaminated Si samples before and after annealing for 30 min at 110 °C with the applied reverse bias of +5 V. In spectra 1 and 3, taken before the RBA, the only trap that can be detected is one with its DLTS peak maximum at about 56 K. The DLTS signatures {activation energy for hole emission (E_h) and pre-exponential factor (A)} for this trap have been determined from Arrhenius plots of T^2 -corrected hole emission rates measured with the use of Laplace DLTS technique as $E_h = 0.10 \pm 0.01$ eV and $A = 1 \times 10^7 \text{ s}^{-1} \text{ K}^{-2}$. These values are close to those reported in the literature for a complex incorporating a substitutional boron atom and an interstitial iron atom (Fe-B).^{1,12,15} Concentrations of the Fe-B defect before any annealing steps were determined using DLTS and in the bulk were $7 \pm 2 \times 10^{11} \text{ cm}^{-3}$ in sample Si-Fe1 (spectrum 1) and $1.3 \pm 0.3 \times 10^{13} \text{ cm}^{-3}$ in sample Si-Fe2 (spectrum 3) with the concentration reducing closer to the surface. Dissociation of the Fe-B complex upon annealing at temperatures higher than 100 °C is known to result in the appearance of single interstitial iron atoms in Fe-contaminated Si samples. Usually, the $\text{Fe-B} \leftrightarrow \text{Fe}_i + \text{B}$ reaction in boron-doped Si is fully reversible and it is a common

approach to consider the concentration of available single interstitial Fe atoms in a Si:B + Fe sample as equal to the concentration of Fe-B complexes measured after a long enough association period at room temperature.^{1,6,7,21} So, in the following, we will refer to the above values of concentrations of Fe-B complexes in the un-annealed Si-Fe1 and Si-Fe2 samples as the initial concentrations of single interstitial Fe atoms, $[\text{Fe}_i]$.

In spectra 2 and 5, recorded after 110 °C RBAs of the Si-Fe1 and Si-Fe2 samples, two other peaks can be seen, one with its maximum at 190 K and the other at 245 K. The DLTS signatures for the trap with its peak maximum at 245 K ($E_h = 0.46 \pm 0.02$ eV and $A = 5 \times 10^6 \text{ s}^{-1} \text{ K}^{-2}$) are close to those reported in the literature for Fe_i .^{1,12,15} The DLTS signatures for the trap with its peak maximum at 190 K ($E_h = 0.31 \pm 0.02$ eV and $A = 9.3 \times 10^5 \text{ s}^{-1} \text{ K}^{-2}$) do not coincide with the values reported for traps in Fe-contaminated p-type Si but are close to those reported in Ref. 16 for a minority carrier trap detected in Fe-contaminated n-type Si and assigned to a Fe-H complex. From Fig. 1, it can be seen that the magnitude of the peak at 190 K is much bigger in spectrum 5 than in spectrum 2. The only difference between the samples, on which spectra 2 and 5 have been recorded, is the Fe_i concentration, so it can be suggested that the defect responsible for the DLTS peak with its maximum at 190 K is related to Fe. When a Si-Fe2 sample was annealed at 110 °C without bias (spectrum 4), there was no peak at 190 K and the magnitude of the peak at 245 K (assigned to Fe_i) was much smaller due to the re-formation of Fe-B pairs during annealing and cooling down.

From comparison of the spectra pairs 1 and 2 and 3 and 5, it might at first appear that the total concentration of defects is higher in the samples subjected to reverse bias annealing. This simple comparison is, however, misleading because it does not take into account changes in the diode capacitance and depletion width due to the dissociation of B-H complexes and redistribution of hydrogen, as well as the very non-uniform concentration profiles of the Fe-related defects, which are shown in Fig. 2.

Fig. 2(a) shows the concentration profiles, determined from CV measurements, of uncompensated shallow acceptor centers (N_a^-) induced by different annealing treatments of a Si-Fe2 sample with initial $[\text{Fe}_i] = 1.3 \times 10^{13} \text{ cm}^{-3}$. The original profile (before annealing) shows a strong drop in N_a^- close to the surface. This is because of the hydrogen passivation of substitutional boron atoms.²⁴ An analysis of the profile indicates that the concentration of the electrically inactive B-H complexes is over 10^{15} cm^{-3} close to the surface. The B-H complexes dissociate at temperatures higher than 100 °C;²⁴ therefore, over 10^{15} cm^{-3} hydrogen atoms can appear in the sub-surface region upon annealing. Fig. 2 shows that reverse bias annealing (110 °C, +5 V, 30 min) has resulted in the hydrogen passivation of boron atoms deeper into the bulk of the silicon sample. This is due to the H atoms being positively charged, and therefore drifting towards the bulk when under reverse bias and forming the B-H complexes when the sample is cooled down. After the 30 min 175 °C anneal with no bias, the hydrogen has been strongly redistributed and its concentration is at least an order of magnitude lower close to the surface (Fig. 2(a)).

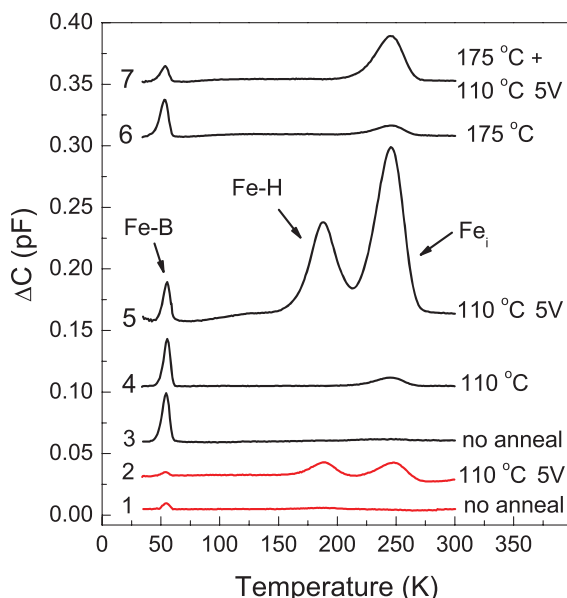


FIG. 1. DLTS spectra of Fe contaminated p-type Cz-Si samples with initial Fe_i concentrations of $7 \times 10^{11} \text{ cm}^{-3}$ (1, 2 in red) and $1.3 \times 10^{13} \text{ cm}^{-3}$ (3–7 in black) taken before any annealing (1,3), after a 110 °C anneal (4), after a 110 °C, +5 V, 30 min RBA (2,5), after a 175 °C 30 min anneal (6), and after a 175 °C 30 min anneal followed by a 110 °C, +5 V, 30 min RBA (7). The measurement conditions were the following: rate window (e_h) = 80 s⁻¹, reverse bias (U_r) = +5 V, filling pulse voltage (U_p) = 0 V, and filling pulse length (t_p) = 1 ms. The peaks in spectra 2 (and 5) are bigger than those in spectra 1 (and 4), due to the change in carrier concentration due to the movement of hydrogen, and do not represent an increase in total Fe concentration.

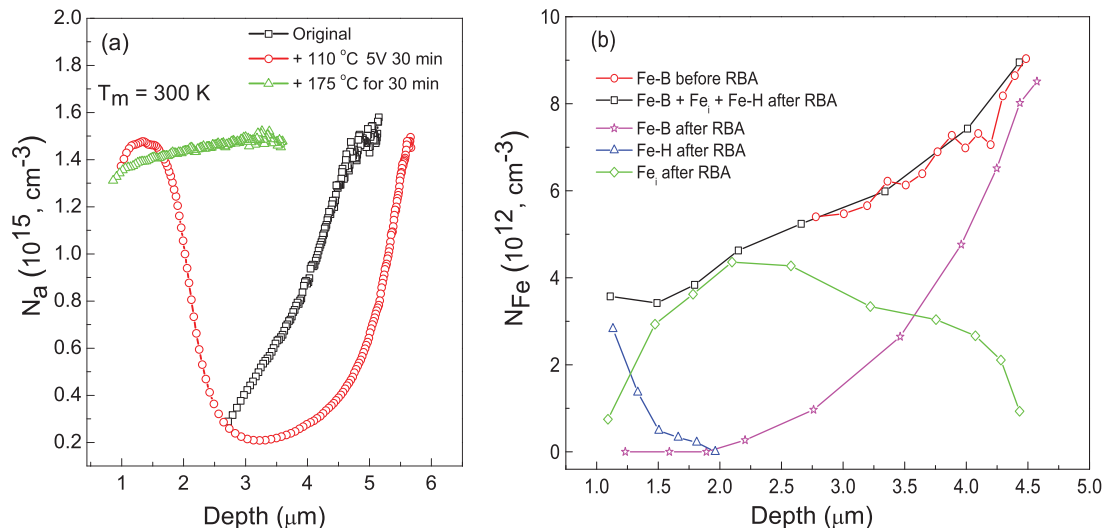


FIG. 2. Concentration depth profiles for Fe contaminated p-type Cz-Si sample with initial $[\text{Fe}_i] = 1.3 \times 10^{13} \text{ cm}^{-3}$ of (a) uncompensated acceptors and (b) Fe-B before a reverse bias anneal, and of Fe-B, Fe_i , and Fe-H after a 110 °C, 30 min, +5 V reverse bias anneal. The combined total of all the Fe related centers after the reverse bias anneal is also plotted.

Spectrum 6 in Fig. 1 has been recorded on a Si-Fe2 sample with initial $[\text{Fe}_i] = 1.3 \times 10^{13} \text{ cm}^{-3}$ after a 30 min 175 °C anneal under no bias. The spectrum shows mainly the Fe-B-related signal and a small signal due to hole emission from Fe_i . Spectrum 7 has been recorded on the same sample after a subsequent reverse bias annealing (110 °C, 30 min, +5 V). No peak at 190 K is observed in the spectrum. The only difference between spectra 5 and 7 in Fig. 1 is that the sample on which spectrum 5 was recorded has much more hydrogen in the sub-surface region. This indicates that the defect giving rise to the DLTS peak at 190 K can only be formed when there is a large amount of H, and, as we have already demonstrated a correlation with the bulk iron concentration, we therefore assign it to a Fe-H complex.

Fig. 2(b) shows the concentration depth profile of the Fe-B complex before reverse bias annealing and the Fe-B, Fe_i , and Fe-H after the RBA. They are derived from CV measurements and LDLTS profiling measurements using a correction based on Debye screening to determine the crossing point of the Fermi level and the trap level (the λ point)²⁵ at 57 K, 190 K, and 250 K, respectively. It can be seen that the Fe-H complex concentration is steeply profiled, rising towards the surface. The reasons for this spatial dependency are not fully understood, but we note here that the Fe-H formation and dissociation reactions are strongly dependent on the position of the Fermi level. In the bulk p-type region, Fe_i is positively charged under the annealing conditions used, making it unlikely that it will react with positively charged H and more likely to form complexes with negatively charged acceptors, in this case substitutional boron. However, in the depletion region, the Fe_i atoms are neutral and can interact with available H atoms forming Fe-H complexes. Under the annealing conditions, the depletion region extends $\sim 2.5 \mu\text{m}$ from the surface and the Fe-H profile is detectable to a depth of $\sim 2 \mu\text{m}$. The Fe-H formation rate and equilibrium concentration of the complex depend on the Fermi level position in the depletion and λ regions as well as the hydrogen supply, and

we hypothesise that these three factors might be responsible for the shape of the profile. By comparing the combined concentrations of Fe-B, Fe_i , and Fe-H after the RBA to the initial concentration of Fe-B before the RBA (Fig. 2(b)), it can be seen that there is no significant change in the total concentration of Fe related centers. This provides further evidence of the center responsible for the DLTS peak at 190 K being associated to a Fe related defect.

Fig. 3(a) shows the conventional DLTS spectra of Si-Fe2 samples with initial $[\text{Fe}_i] = 1.3 \times 10^{13} \text{ cm}^{-3}$ annealed for 30 min under +5 V reverse bias at different temperatures in the range from 80 to 120 °C. The DLTS signal due to the Fe-H complex can be seen to appear after a 90 °C RBA and has its highest magnitude after the 110 °C RBA. The peak then starts to diminish after a 120 °C RBA. In the DLTS spectra of samples subjected to RBAs above 130 °C, the Fe-H complex is not observed at all. The small temperature window and the requirement of annealing under reverse bias for the formation and existence of the Fe-H complex explain why it has not been observed before. A similar material and similar annealing conditions to those chosen by us were used in Ref. 13, but the Fe-H complex was not observed in that study. In that work, wet chemical etching was used to introduce hydrogen and the authors measured less than 10^{14} cm^{-3} hydrogen atoms in the subsurface region, which appears not to be enough to create Fe-H complexes. Fig. 3(b) shows how 30 min isochronal anneals under no bias effect, and the Fe-H complex created upon reverse bias annealing at 110 °C. The complex can be seen to disappear completely after a 125 °C anneal.

An analysis of the total concentration of all electrically active Fe_i -related traps (Fe_i , $\text{Fe}_i\text{-B}$, and $\text{Fe}_i\text{-H}$) calculated by summing the individual contributions determined from the magnitudes of all three DLTS peaks before and after the different annealing steps has shown that there is no significant change in the total number of the Fe_i related centers and therefore it does not appear that some Fe atoms have been

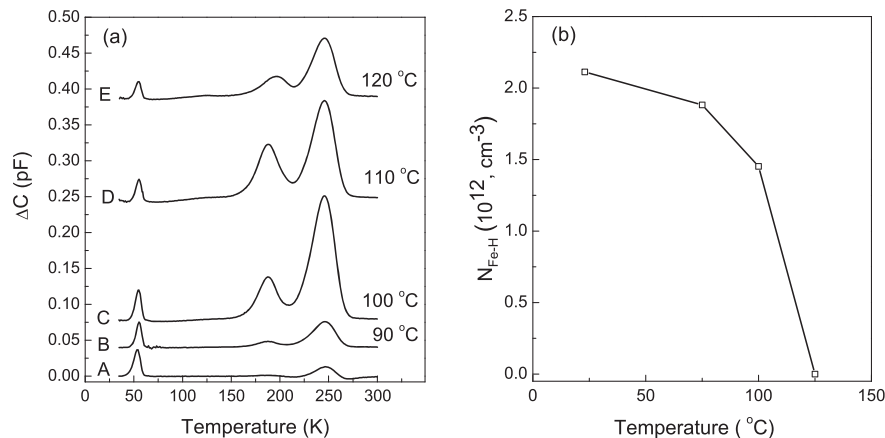


FIG. 3. (a) DLTS spectra of Fe contaminated p-type Cz-Si sample with initial $[Fe_i] = 1.3 \times 10^{13} \text{ cm}^{-3}$ taken after a 30 min +5 V RBA at (A) 80 °C, (B) 90 °C, (C) 100 °C, (D) 110 °C, and (E) 120 °C. The measurement conditions were the following: $(e_h) = 80 \text{ s}^{-1}$, $(U_r) = +5 \text{ V}$, $(U_p) = 0 \text{ V}$, and $(t_p) = 1 \text{ ms}$. (b) Changes in concentration of the Fe-H complex upon 30 min isochronal annealing without bias of a Fe contaminated p-type Cz-Si sample with initial $[Fe_i] = 1.3 \times 10^{13} \text{ cm}^{-3}$ after creation of the complex by a 30 min, 110 °C, +5 V reverse bias anneal. The given values of Fe-H concentration are averaged concentrations of the complex in the range of 1.3–2.0 μm below the surface.

completely electrically passivated. Determining the composition (number of hydrogen atoms incorporated and structure) of the detected Fe-H complex with the use of CV and DLTS measurements is a difficult task. The *ab initio* calculations predict that H does not bind with Fe-B pairs and the most energetically favorable Fe-H complex consists of a Fe atom at a hexagonal lattice site with a hydrogen atom bonded to the Fe atom.¹⁷ The activation energy for hole emission from the Fe-H trap determined from an Arrhenius plot of T^2 corrected emission rates has been found to be 0.31 eV, which is in close agreement to the hole ionization energy for a donor level of the Fe-H complex found by *ab initio* calculations.¹⁷ Direct hole capture cross section measurements have been carried out and show that the capture cross section (σ) is not temperature dependent and its value is $5.2 \times 10^{-17} \text{ cm}^2$. The σ value is within the range of capture cross sections for capture of charge carriers by neutral centers, confirming the donor nature of the level.

A consideration of the electronic properties of Fe_i and H atoms in silicon suggests that these atoms are unlikely to form a pair in the bulk of p-type Si because of their Coulomb repulsion.²⁶ In the recent study by Liu *et al.*,¹⁹ an almost complete passivation of Fe_i by hydrogen has been reported. The authors have suggested that annealing at 700 °C can form negatively charged hydrogen atoms which can then pair with positively charged Fe_i to form stable Fe-H complexes in multi-crystalline silicon. However, our results suggest that the Fe-H complex generated during our experiments would dissociate at such high temperatures. Further, the Fe-H complex we have observed has a deep donor level within the band gap, so it can be an effective recombination center. It would seem that the strong decrease in $[Fe_i]$ observed by Liu *et al.* upon hydrogen introduction at much higher temperatures than we have used could be associated with the formation of a different complex with hydrogen or some other mechanism is involved.

To conclude, we have presented evidence for a Fe-H complex forming in Fe-contaminated p-type Czochralski silicon upon reverse bias annealing in the temperature range of

90–120 °C. The complex only forms when there are large amounts of H and its concentration is related to the concentration of Fe_i in the samples. The complex has a deep donor level at $E_V + 0.31 \text{ eV}$ which is in a good agreement with the value predicted by *ab initio* calculations¹⁷ and has a direct hole capture cross section of $5.2 \times 10^{-17} \text{ cm}^2$. The complex can be seen to disappear completely after a 125 °C anneal for 30 min. No evidence of total electrical passivation of Fe due to the incorporation of hydrogen has been obtained in this work.

We would like to thank EPSRC (UK) for funding this work via Grant No. EP/K006975/1 at Manchester and via Grant No. EP/J01768X/2 at Warwick.

- ¹A. A. Istratov, H. Hieslmair, and E. R. Weber, *Appl. Phys. A* **69**, 13 (1999).
- ²G. Coletti, R. Kvande, V. D. Mihailetschi, L. J. Geerligs, L. Arnberg, and E. J. Ovreliid, *J. Appl. Phys.* **104**, 104913 (2008).
- ³R. Kvande, L. J. Geerligs, G. Coletti, L. Arnberg, M. Di Sabatino, E. J. Ovreliid, and C. C. Swanson, *J. Appl. Phys.* **104**, 064905 (2008).
- ⁴S. K. Estreicher, M. Sanati, and N. G. Szwacki, *Solid State Phenom.* **131**, 233 (2007).
- ⁵K. Wunstel and P. Wagner, *Solid State Commun.* **40**, 797 (1981).
- ⁶G. Zoth and W. Bergholz, *J. Appl. Phys.* **67**, 6764 (1990).
- ⁷W. Wijaranakula, *J. Electrochem. Soc.* **140**, 275 (1993).
- ⁸J. Hofstetter, J. F. Lelièvre, C. del Cañizo, and A. Luque, *Mater. Sci. Eng., B* **159–160**, 299 (2009).
- ⁹S. P. Phang and D. Macdonald, *J. Appl. Phys.* **109**, 073521 (2011).
- ¹⁰A. R. Peaker, V. P. Markevich, B. Hamilton, G. Parada, A. Dudas, A. Pap, E. Don, B. Lim, J. Schmidt, L. Yu, Y. Yoon, and G. Rozgonyi, *Phys. Status Solidi A* **209**, 1884 (2012).
- ¹¹F. Jiang, M. Stavola, A. Rohatgi, D. Kim, J. Holt, H. Atwater, and J. Kalejs, *Appl. Phys. Lett.* **83**, 931 (2003).
- ¹²S. J. Pearton and A. J. Tavendale, *J. Phys. C: Solid State Phys.* **17**, 6701 (1984).
- ¹³O. V. Feklisova, A. L. Parakhonsky, E. B. Yakimov, and J. Weber, *Mater. Sci. Eng., B* **71**, 268 (2000).
- ¹⁴M. Kouketsu and S. Isomae, *J. Appl. Phys.* **80**, 1485 (1996).
- ¹⁵C. K. Tang, L. Vines, B. G. Svensson, and E. V. Monakhov, *Appl. Phys. Lett.* **99**, 052106 (2011).
- ¹⁶T. Sadoh, K. Tsukamoto, A. Baba, D. Bai, A. Kenjo, T. Tsurushima, H. Mori, and H. Nakashima, *J. Appl. Phys.* **82**, 3828 (1997).
- ¹⁷M. Sanati, N. Szwacki, and S. Estreicher, *Phys. Rev. B* **76**, 125204 (2007).

- ¹⁸B. J. Hallam, P. G. Hamer, S. R. Wenham, M. D. Abbott, A. Sugianto, A. M. Wenham, C. E. Chan, G. Xu, J. Kraiem, J. Degoulange, and R. Einhaus, *IEEE J. Photovoltaics* **4**, 88 (2014).
- ¹⁹A. Liu, C. Sun, and D. Macdonald, *J. Appl. Phys.* **116**, 194902 (2014).
- ²⁰P. Karzel, A. Frey, S. Fritz, and G. Hahn, *J. Appl. Phys.* **113**, 114903 (2013).
- ²¹J. D. Murphy and R. J. Falster, *Phys. Status Solidi RRL* **5**, 370 (2011).
- ²²J. D. Murphy and R. J. Falster, *J. Appl. Phys.* **112**, 113506 (2012).
- ²³L. Dobaczewski, P. Kaczor, I. D. Hawkins, and A. R. Peaker, *J. Appl. Phys.* **76**, 194 (1994).
- ²⁴C. T. Sah, *Appl. Phys. Lett.* **43**, 204 (1983).
- ²⁵D. Stievenard and D. Vuillaume, *J. Appl. Phys.* **60**, 973 (1986).
- ²⁶T. Heiser and A. Mesli, *Phys. Rev. Lett.* **68**, 978 (1992).